

Table S1: Concentration of elements in AWF.

Element	Conc. (ppm)^a	Std Dev. (ppm)	Conc. (M)^b	Std Dev. (M)
Ca	389.1	44.9	9.7 mM	1.1 mM
K	1250.7	210.5	32 mM	5.4 mM
Mg	107.8	7.5	4.4 mM	0.3 mM
Na	25.7	6.1	1.1 mM	0.3 mM
P	36.9	10.4	1.2 mM	0.3 mM
S	247.3	82.8	7.7 mM	2.6 mM
B	2.8	0.9	258.5 μ M	80.4 μ M
Fe	0.12	0.02	2.16 μ M	0.4 μ M
Mn	2.6	0.2	47.5 μ M	3.1 μ M
Zn	0.44	0.03	6.7 μ M	0.5 μ M
Cd	0.008	0.001	66.7 nM	12.4 nM

a. Concentration of element given in parts per million

b. Concentration of element given in molarity

Table S2: Primers used in this study.

Primer	Sequence (5'-3')	Description
oSWC01445	ATGCTTCCGGCTCGTATGTTGT GT	Forward M13 primer
oSWC01446	GGCGATTAAGTTGGGTAACGC CAG	Reverse M13 primer
oSWC01662	TCGTTGATCGCGGTCGCCACC	Downstream forward <i>cvsS</i> KO
oSWC01663	CACATGGAATTCTTTCCGAGC GTTGCGCCTGC	Downstream forward nested <i>cvsS</i> KO with EcoRI site
oSWC01664	ATTGACCTGCCGGAACGTACC	Downstream reverse <i>cvsS</i> KO
oSWC01665	GGTACGTTCCGGCAGGTCAAT CAACCGCCTTTGTATGGACTTC	Upstream forward <i>cvsS</i> KO with overlap
oSWC01666	TGATGCGCAGGATATTGAGTG G	Upstream reverse <i>cvsS</i> KO
oSWC01667	CACATGGGATCCAGCGTCTCT GTGCCATCCTTGG	Upstream nested reverse <i>cvsS</i> KO with BamHI site
oSWC01668	TCGTCGTC AATCAACAGGC	Downstream forward <i>cvsR</i> KO
oSWC01669	CACATGGAATTCAAACGCACC TCGCTATCGGC	Downstream forward nested <i>cvsR</i> KO with EocRI site
oSWC01670	TATCTTTACGGTGGAGCCGGG G	Downstream reverse <i>cvsR</i> KO
oSWC01671	CGGCTCCACCGTAAAGATATT CAACCAGTAACAGGCGCATC	Upstream forward <i>cvsR</i> KO with overlap
oSWC01672	TGTCTGTCAGTGCCACCAG	Upstream reverse <i>cvsR</i> KO
oSWC01673	CACATGGGATCCTTCGCTTAG GCAGGGAAGG	Upstream nested reverse <i>cvsR</i> KO with BamHI site
oSWC01700	TTGGGCACAGGTTTCGGTCTTG	Downstream forward PCR screen <i>cvsS</i> KO
oSWC01701	AAGCACCAGTCCTGATGGC	Downstream reverse PCR screen <i>cvsS</i> KO
oSWC01702	TTGAGTCCGGCAGACTCCAGC	Upstream forward PCR screen <i>cvsS</i> KO
oSWC01703	TAAGGGTCTGGCGACACCG	Upstream reverse PCR screen <i>cvsS</i> KO
oSWC01704	AGCAAGTGGTTGATCTGGG	Downstream forward PCR screen <i>cvsR</i> KO and used in RT-PCR for <i>cvsR-cvsS</i>
oSWC01705	ATCACGGTGCGCAGGGCGCTT C	Downstream reverse PCR screen <i>cvsR</i> KO
oSWC01706	TGATTCCTGTAGACCTGGC	Upstream forward PCR screen <i>cvsR</i> KO
oSWC01707	ATGCCAAAGCACTGAGCAAG	Upstream reverse PCR screen <i>cvsR</i> KO

oMRF0150	GCCTTGCGGGGTCAACAA	Reverse for RT-PCR for PSPTO_3383-PSPTO_3382
oSWC05046	GACAAGCGTCTCTGTGCCATCCT	Forward primer for RT-PCR for PSPTO_3382- <i>cvsR</i>
oMRF0145	GGCCAGGTCTACAGGAATCATC	Forward primer for RT-PCR for PSPTO_3383-PSPTO_3382
oMRF0148	GGTGTCGCCAGACCCTTACC	Reverse primer for RT-PCR for PSPTO_3382- <i>cvsR</i>
oMRF0535	GGCGTGCGGTGATCGAG	Reverse primer for RT-PCR for <i>cvsR-cvsS</i>
oMRF0010	CACCGTTTTTCATTGTTAGGAGGGTCCATAG	reverse promoter fusion without PSPTO_3383 gene, begins at end of PSPTO_3383
oMRF0011	TGTCGTAATGCTGTGTCTGTCA GTG	forward promoter fusion 400bp upstream of PSPTO_3383
oMRF0016	GCGGCTTAACTCAAGCGTTAG A	forward primer for pBS59
oMRF0017	TCCTGAGGTAGCCATTCATCC A	reverse primer for pBS59
oMRF0050	TCACTTGTCATCGTCGTCCTTG TAGTCACCCCCGGCTCCACCG	C-terminal FLAG-tag gateway overexpression C-terminus of <i>cvsR</i>
oMRF0051	CACCATGCGCCTGTTACTGGTT GAAG	C-terminal FLAG-tag gateway overexpression N-terminus of <i>cvsR</i>
oMRF0233	CAAGCGTCTCTGTGCCATC	<i>algD</i> qPCR sense
oMRF0234	CGAGCGGAAGAATGACACC	<i>algD</i> qPCR antisense
oSWC02061	TTTCTGCAGCAACCGCCTTTGT ATGG	<i>cvsR</i> complement forward primer
oSWC02063	TTTAAGCTTTTGGCATGTTTTT GATGG	<i>cvsR</i> complement reverse primer
oMRF0355	CGGCGGCCGCCGCCTTTGTAT GGACTTCAACC	Reverse primer for <i>cvsR</i> insertion into pET21 with NotI site
oMRF0357	CGGGATCCATGCGCCTGTTAC TGGTTGAA	Forward primer for <i>cvsR</i> insertion into pET21 with BamHI site
oMRF0375	CTGTAAGCGCTTGTTTCGCATT	<i>hrpR</i> peak #2 ChIP-seq peak 5'-FAM tag for EMSA and DNase footprinting
oMRF0376	AGAAACGCGCTATTCATTGCA	<i>hrpR</i> peak #2 ChIP-seq peak 3' for EMSA and DNase footprinting
oMRF0377	TGCGGAGTAAATCGCAGGC	<i>spf</i> ChIP-seq peak 5'-FAM tag for EMSA and DNase footprinting
oMRF0378	GCAGTGCCGCTGCTGGT	<i>spf</i> ChIP-seq peak 3' for EMSA and DNase footprinting

oMRF0381	TGCAGGCGTCGAGTCTAACA	PSPTO_3383 ChIP-seq peak 5'-FAM tag for EMSA and DNase footprinting
oMRF0382	TGCGGATCGATGCCACG	PSPTO_3383 ChIP-seq peak 3' for EMSA and DNase footprinting
oMRF0385	GCAAGTGTCAATATTGAGTTGACTCAAC	PSPTO_0203 ChIP-seq peak 5' for EMSA and DNase footprinting
oMRF0386	CCTTGATGCTTCCACCAGGA	PSPTO_0203 ChIP-seq peak 3' with 5'FAM for EMSA and DNase footprinting
oMRF0387	TGGCCGTTATTTAACGCATTG	<i>katB</i> ChIP-seq peak 5'-FAM for EMSA and DNase footprinting
oMRF0388	GCGCGACGTTAAGAGTGCA	<i>katB</i> ChIP-seq peak 3' for EMSA and DNase footprinting
oMRF0389	CCTTACGCAGCCCGTGAG	tRNA-cys-1 ChIP-seq peak 5'-FAM for EMSA and DNase footprinting
oMRF0390	GCCGAGGTCGGAATCGAA	tRNA-cys-1 ChIP-seq peak 3' for EMSA and DNase footprinting
oMRF0391	GGCATCGACCTTGTCAGATCC	PSPTO_4969 ChIP-seq peak 5' for EMSA and DNase footprinting
oMRF0392	TATGGTTTCCCGGTCAAGGACACGAAAATCTTCATCGAGTGA	PSPTO_4969 ChIP-seq peak 3' w/ 5'FAM tag for EMSA and DNase footprinting
oMRF0393	AGCTGTGGAAACTCGCGAA	<i>gidA</i> ChIP-seq peak 5' for EMSA and DNase footprinting
oMRF0394	CGGACTTGATCGCTGGCTT	<i>gidA</i> ChIP-seq peak 3' with 5' FAM tag for EMSA and DNase footprinting
oMRF0395	TCATCCGTTAAATCCCATCTG	<i>oprF</i> ChIP-seq peak 5'-FAM for EMSA and DNase footprinting
oMRF0396	GCGCTAGCGCTCAAGGGA	<i>oprF</i> ChIP-seq peak 3' for EMSA and DNase footprinting
oKMD0123	TGTCACTCTTGTAACGAACTTG	PSPTO_5255 3' FAM-tag for EMSA and DNase footprinting
oMRF0062	GCCATCACCTAGAATGT	PSPTO_5255 5' for EMSA and DNase footprinting
oKMD0137	CGAACAACACAGAGGCTTGGA	<i>hrpR</i> peak #1 3' FAM-tag for EMSA and DNase footprinting
oSWC06572	TAC	<i>hrpR</i> peak #1 5' for EMSA and DNase footprinting
oMRF0191	CGCTCAAAGTACCAATC	<i>fliC</i> qPCR sense

oMRF0192	GCTCAAAGTCAGAGAGA	<i>fliC</i> qPCR antisense
oMRF0231	GGATAACAAGGCGTAAA	<i>hopAH2-1</i> qPCR sense
oMRF0232	GCCTGATTCAACTTGTC	<i>hopAH2-1</i> qPCR antisense
oSWC06118	GTGCCAACGGACAGGCACA	<i>rsmZ</i> qPCR sense
oSWC06119	CCCTTGTCATCGTCCTGATGAA	<i>rsmZ</i> qPCR antisense
oSWC06338	GCAGGAAGCGCAACAAGACA T	<i>rsmY</i> qPCR sense
oSWC06339	GCTTTCCAGACTGTTTCCCTGA T	<i>rsmY</i> qPCR antisense
oSWC06348	GGTGAACAAGGAGTTCACCAG GA	<i>rsmX-3</i> qPCR sense
oSWC06349	CCAAGACCATTCCAACCTCCCT GT	<i>rsmX-3</i> qPCR antisense

Table S3: Strains and plasmids used in this study.

Strain Name	Genotype	Reference
<i>Pseudomonas syringae</i> pv. <i>tomato</i> DC3000 strains		
<i>Pto</i> (WT)	<i>Pseudomonas syringae</i> pv. <i>tomato</i> DC3000 wild type, Rif ^R	(1)
BBPS33	<i>Pto</i> Δ <i>cvsS</i>	(2)
BBPS34	<i>Pto</i> Δ <i>cvsR</i>	(2)
BBPS35	BBPS34 <i>attTn7::Tn7-PSPTO_3383-cvsR</i>	(2)
MFPS03	<i>Pto</i> pBS59:: <i>P_{cvsSR}</i>	This study
MFPS04	<i>Pto</i> Δ <i>cvsS</i> pBS59:: <i>P_{cvsSR}</i>	This study
MFPS04	<i>Pto</i> Δ <i>cvsR</i> pBS59:: <i>P_{cvsSR}</i>	This study
BMS2	<i>Pto</i> pBS44	(3)
PS392	<i>Pto</i> Δ <i>algD</i>	(4)
MFPS10	<i>Pto</i> Δ <i>algD</i> Δ <i>cvsS</i>	This study
MFPS11	<i>Pto</i> Δ <i>algD</i> Δ <i>cvsR</i>	This Study
CUCPB5113	<i>Pto</i> Δ <i>hrcQb-U</i> , Sp ^R	(5)
MFPS05	<i>Pto</i> Δ <i>hrcQb-U</i> Δ <i>cvsS</i> , Sp ^R	This study
MFPS06	<i>Pto</i> Δ <i>hrcQb-U</i> Δ <i>cvsS</i> , Sp ^R	This study
MFPS09	<i>Pto</i> Δ <i>cvsR</i> pBS46:: <i>cvsR-FLAG</i>	This study
MFPS20	<i>Pto</i> pBS58:: <i>P_{hrpRS}</i>	This study
MFPS21	<i>Pto</i> Δ <i>cvsS</i> pBS58:: <i>P_{hrpRS}</i>	This study
MFPS22	<i>Pto</i> Δ <i>cvsR</i> pBS58:: <i>P_{hrpRS}</i>	This study
MFPS24	<i>Pto</i> pBS63	This study
MFPS25	<i>Pto</i> Δ <i>cvsS</i> pBS63	This study
MFPS26	<i>Pto</i> Δ <i>cvsR</i> pBS63	This study
<i>Escherichia coli</i> strains		
DH5 α	<i>huA2 lac(del)U169 phoA glnV44 Φ80' lacZ(del)M15 gyrA96 recA1 relA1 endA1 thi-1 hsdR17</i>	ThermoFisher Scientific
TOP10	F- <i>mcrA</i> Δ (<i>mrr-hsdRMS-mcrBC</i>) Φ 80 <i>lacZ</i> Δ M15 Δ <i>lacX74 recA1 araD139 Δ(ara leu) 7697 galU galK</i> rpsL (StrR) <i>endA1 nupG</i>	ThermoFisher Scientific

BL21 (DE3)		<i>fhuA2 [lon [dcm] Δhs ΔEcoRI-B int::(lacI:: i21 Δnin5</i>
Plasmids		
Name	Description	Reference
pK18mobSacB	pMB1 <i>mob sacB</i> , sucrose ^S , Km ^R	(6)
pZB20	pK18mobSacB with regions flanking PSPTO_3380 cloned into it using the EcoRI-BamHI site	(2)
pZB21	pK18mobSacB with regions flanking PSPTO_3381 cloned into it using the EcoRI-BamHI site	(2)
pENTR/D/TOPO	Directional cloning vector for entry to the Gateway System	ThermoFisher Scientific
pENTR/SD/TOPO	Directional cloning vector with ribosome binding site for entry to the Gateway System	ThermoFisher Scientific
pMRF2	pENTR/D/TOPO::P _{<i>cvsSR</i>}	This study
pBS58	luxCDABE destination vector	(3)
pBS59	luxCDABE destination vector	(3)
pMRF11	pBS59::P _{<i>cvsSR</i>}	This study
pBS44	luxCDABE destination vector control without insertion	(3)
pUC18miniTn7	mini-Tn7 mobilizable transposon with multicloningsite, GmR	(7)

pNTS2	mini-Tn7 helper plasmid	(7)
pJZ1	pUC18miniTn7::PSPTO_3383-cvsR	This study
pBS46	<i>nptII</i> destination vector	(8)
pMRF14	pENTR/SD/TOPO::cvsR-FLAG	
pMRF15	pBS46::cvsR-FLAG	This study
pET21	Bacterial expression vector with T7 lac promoter, N-terminal T7 epitope tag, and C-terminal His tag, ApR	Novagen
pMRF21	pET21::cvsR	This study
pMRF22	pBS58::P _{hrpRS}	This Study
pBS63	pBS58::P _{hrpL}	(9)

- Buell CR, Joardar V, Lindeberg M, Selengut J, Paulsen IT, Gwinn ML, Dodson RJ, Deboy RT, Durkin AS, Kolonay JF, Madupu R, Daugherty S, Brinkac L, Beanan MJ, Haft DH, Nelson WC, Davidsen T, Zafar N, Zhou L, Liu J, Yuan Q, Khouri H, Fedorova N, Tran B, Russell D, Berry K, Utterback T, Van Aken SE, Feldblyum TV, D'Ascenzo M, Deng W-L, Ramos AR, Alfano JR, Cartinhour S, Chatterjee AK, Delaney TP, Lazarowitz SG, Martin GB, Schneider DJ, Tang X, Bender CL, White O, Fraser CM, Collmer A.** 2003. The complete genome sequence of the *Arabidopsis* and tomato pathogen *Pseudomonas syringae* pv. *tomato* DC3000. *Proceedings of the National Academy of Sciences* **100**:10181-10186.
- Butcher BG, Bronstein PA, Myers CR, Stodghill PV, Bolton JJ, Markel EJ, Filiatrault MJ, Swingle B, Gaballa A, Helmann JD, Schneider DJ, Cartinhour SW.** 2011. Characterization of the Fur regulon in *Pseudomonas syringae* pv. *tomato* DC3000. *J Bacteriol* **193**:4598-4611.
- Markel E, Maciak C, Butcher BG, Myers CR, Stodghill P, Bao Z, Cartinhour S, Swingle B.** 2011. An extracytoplasmic function sigma factor-mediated cell surface signaling system in *Pseudomonas syringae* pv. *tomato* DC3000 regulates gene expression in response to heterologous siderophores. *J Bacteriol* **193**:5775-5783.
- Markel E, Stodghill P, Bao Z, Myers CR, Swingle B.** 2016. AlgU Controls Expression of Virulence Genes in *Pseudomonas syringae* pv. *tomato* DC3000. *J Bacteriol* **198**:2330-2344.
- Badel JL, Shimizu R, Oh H-S, Collmer A.** 2006. A *Pseudomonas syringae* pv. *tomato* *avrE1/hopM1* Mutant Is Severely Reduced in Growth and Lesion Formation in Tomato. *Molecular Plant-Microbe Interactions* **19**:99-111.
- Schafer A, Tauch A, Jager W, Kalinowski J, Thierbach G, Puhler A.** 1994. Small mobilizable multi-purpose cloning vectors derived from the *Escherichia coli* plasmids

pK18 and pK19: selection of defined deletions in the chromosome of *Corynebacterium glutamicum*. *Gene* **145**:69-73.

7. **Choi KH, Schweizer HP.** 2006. mini-Tn7 insertion in bacteria with single attTn7 sites: example *Pseudomonas aeruginosa*. *Nat Protoc* **1**:153-161.
8. **Swingle B, Thete D, Moll M, Myers CR, Schneider DJ, Cartinhour S.** 2008. Characterization of the PvdS-regulated promoter motif in *Pseudomonas syringae* pv. *tomato* DC3000 reveals regulon members and insights regarding PvdS function in other pseudomonads. *Molecular Microbiology* **68**:871-889.
9. **McCraw SL, Park DH, Jones R, Bentley MA, Rico A, Ratcliffe RG, Kruger NJ, Collmer A, Preston GM.** 2016. GABA (γ -Aminobutyric Acid) Uptake Via the GABA Permease GabP Represses Virulence Gene Expression in *Pseudomonas syringae* pv. *tomato* DC3000. *Molecular Plant-Microbe Interactions* **29**:938-949.

Figure S1

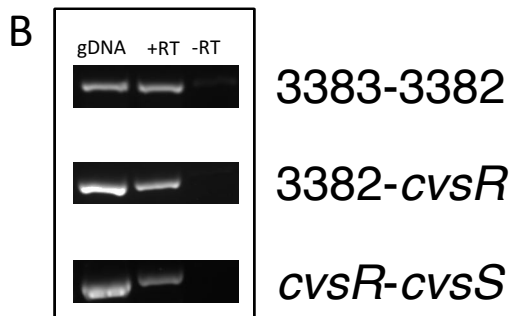
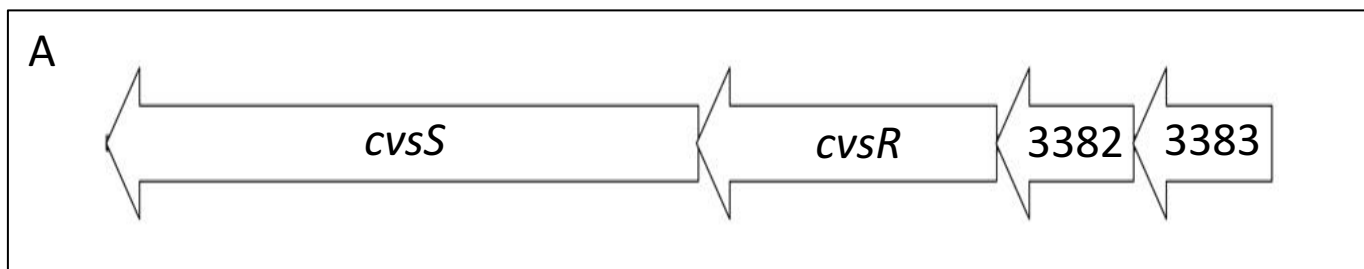


Fig. S1: (A) Genomic arrangement of operon where *cvsS* and *cvsR* are located. (B) Bands produced by PCR of primers overlapping the junction between 3383 and 3382, 3382 and 3381, and 3381 and 3380 using either *Pto* genomic DNA (gDNA), cDNA produced by reverse transcription with random hexamers of RNA (+RT), or a no reverse transcriptase control reaction (-RT). RNA was extracted from *Pto* grown for 18 hours on NB supplemented with CaCl_2 and sodium succinate.

Figure S2

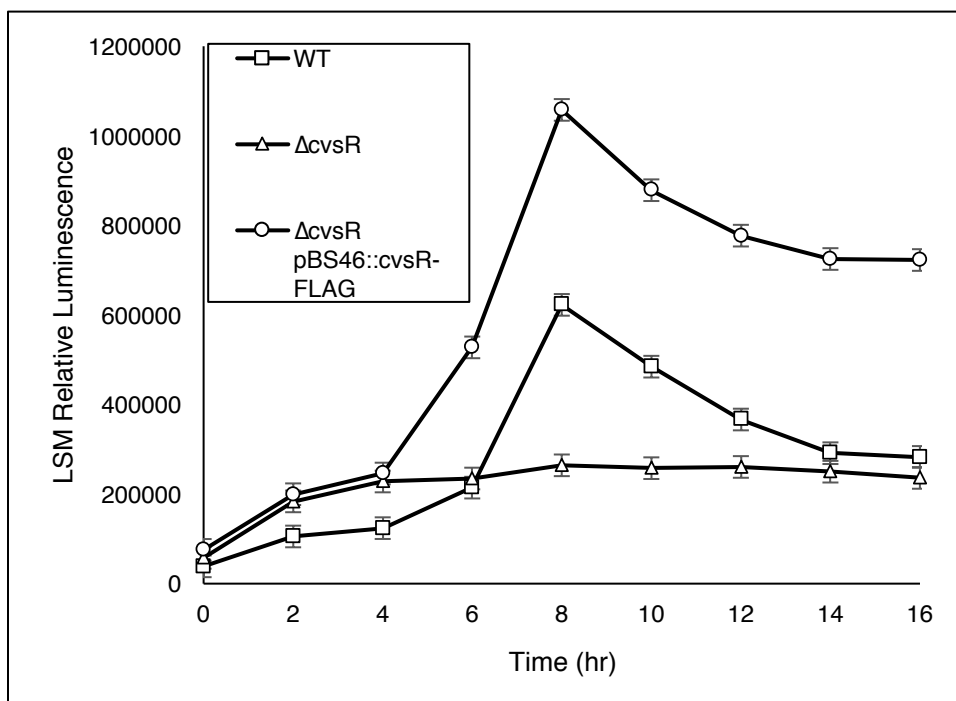


Fig. S2: Luminescence assay to assess transcription of P_{cvsSR} WT, $\Delta cvsR$, and $\Delta cvsR$ pBS46::cvsR-FLAG when grown in MG supplemented with Ca^{2+} . The relative luminescence was calculated using the total luminescence relative to the OD_{600} . This experiment was repeated with independent replicates three times and the three independent experiments were compiled using a least-squares regression. The error bars represent standard error generated by the differences observed between samples.

Figure S3

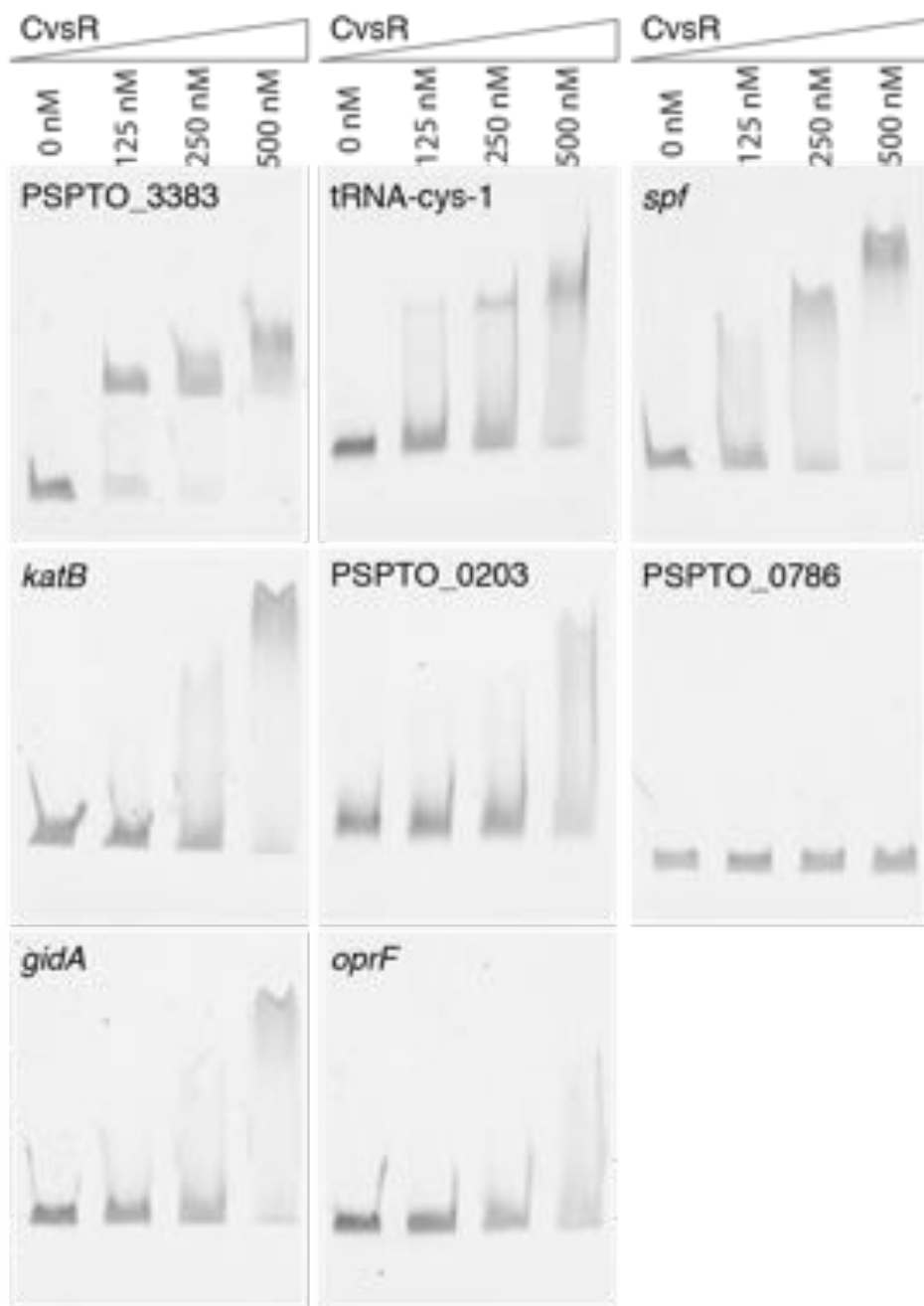


Fig. S3: EMSA with concentrations of CvsR increasing from left to right as written. Probes were chosen based on the location of ChIP-seq peaks, except for PSPTO_3383 and PSPTO_0786. No peak was found near either of those areas in the chromosome. CvsR was predicted to bind upstream of PSPTO_3383 since CvsSR autoregulates. The probe for PSPTO_0786 is used as a negative control. Probes show a shift with an increased concentration of CvsR due to reduced mobility of the probes upon binding of CvsR. This is not seen for the probe for PSPTO_0786.

Figure S4

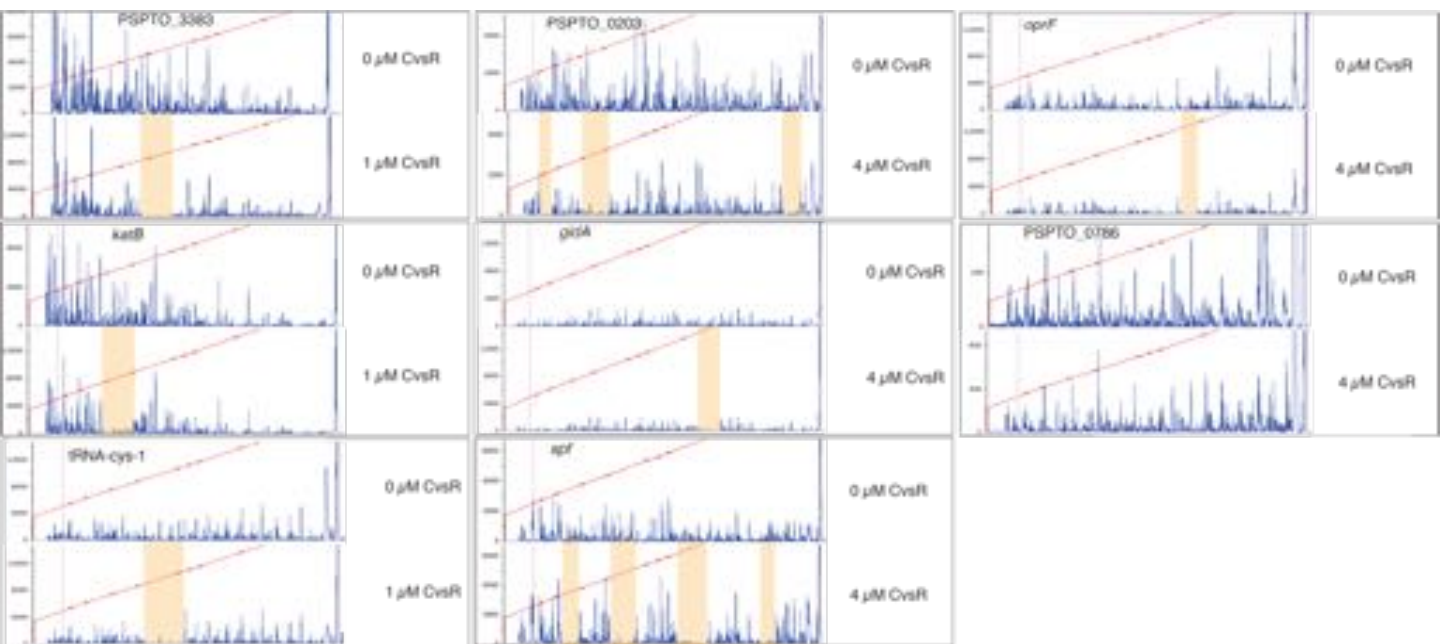


Fig. S4: Fluorescent, non-radioactive DNase footprinting assays showing binding of CvsSR. The red line is a line of best fit that estimates the bp size of each fragment made using a LIZ500 ladder. The blue peaks are fluorescent signal and represent the size of fragmented DNA. The areas that are highlighted in orange are regions with little fluorescence when CvsR is added at 1 μ M or 4 μ M to the reaction as compared to when no CvsR is added. These regions signify areas in the probes that were bound by CvsR. A probe for the region PSPTO_0786 was used as a negative control. There were not any regions that CvsR bound to in this probe.

Figure S6

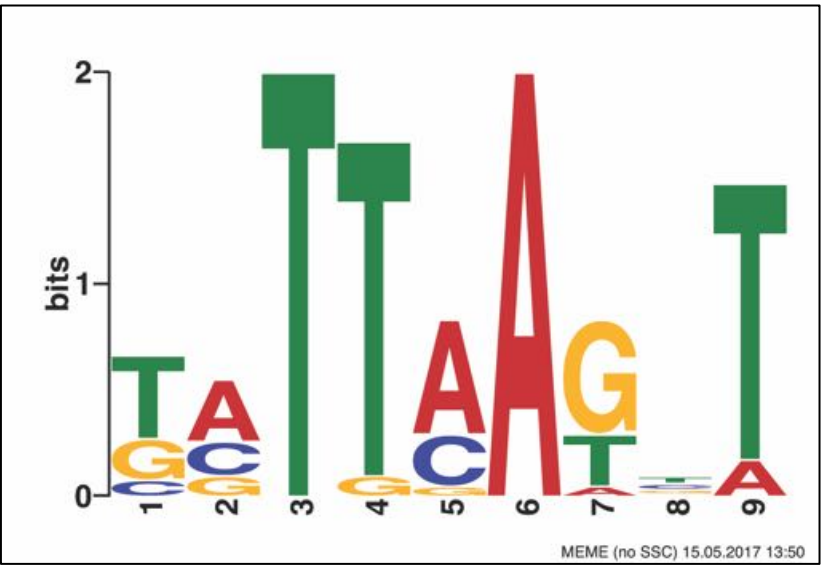


Fig. S6: The predicted binding motif for CvsR discovered using MEME from the compiled Dnase footprinting data.

Figure S7

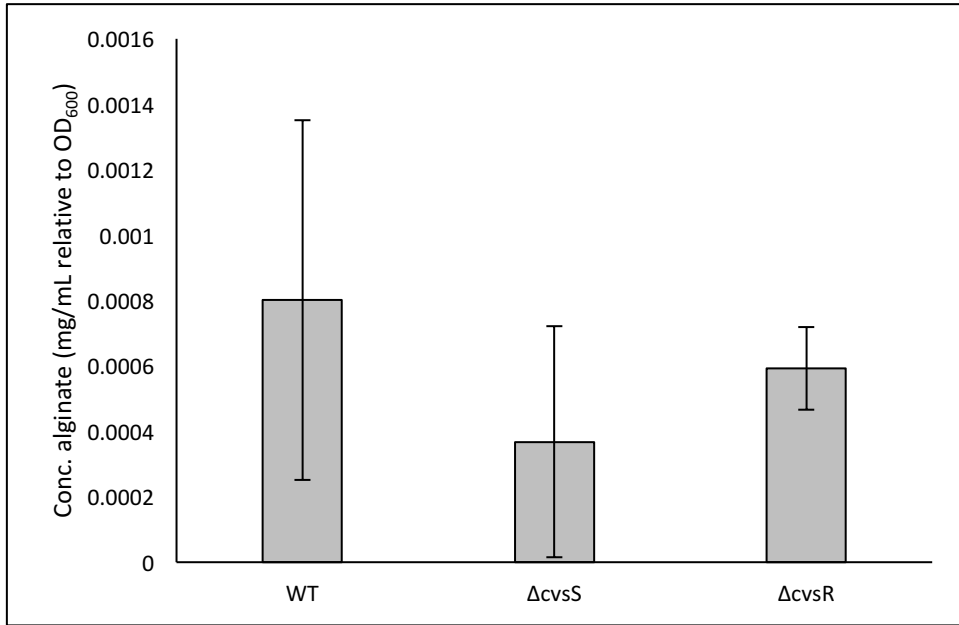


Fig S7: Concentration of alginate produced by WT, $\Delta cvsS$, and $\Delta cvsR$ after one day of growth on NB agar plates. The experiment was repeated using four independent biological replicates. Error bars represent standard deviation between replicates.

Figure S8

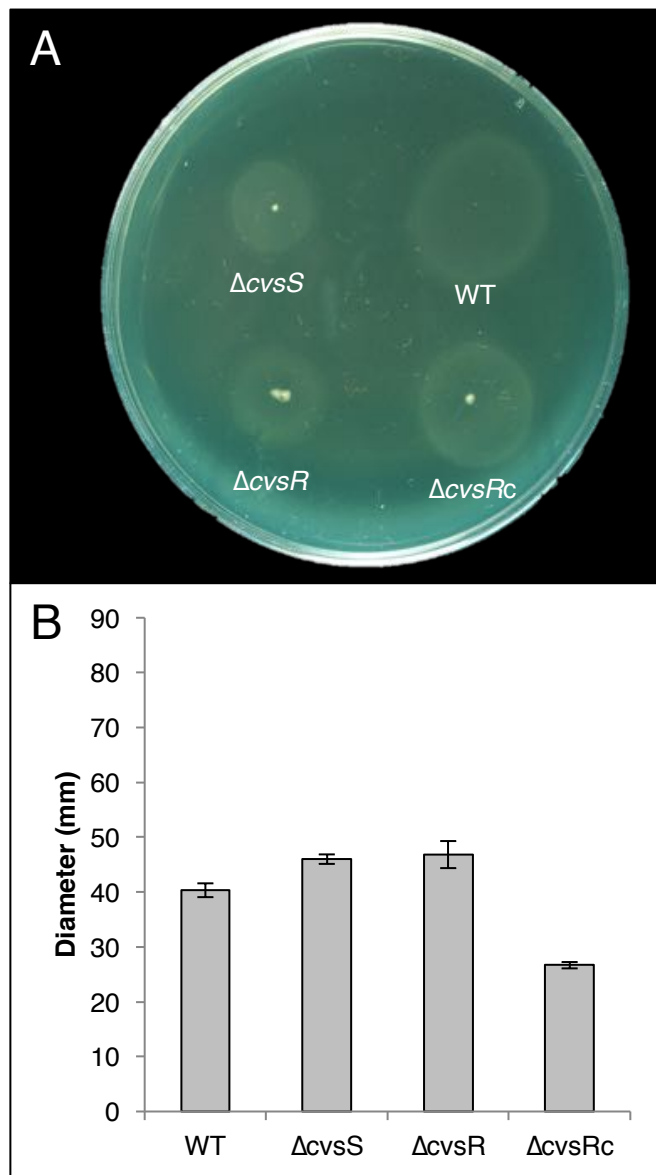


Fig S8: (A) Swarming assays of WT, ΔcvS , ΔcvR , and $\Delta cvRc$ strains grown on NB medium. Pictures of swarming assays taken a day after spotting. (B) Diameters of swarming colonies measured 24 hours after spotting on NB with 5 mM $CaCl_2$. The experiment was performed three times with three replicates per experiment. Diameter of colonies was measured across two locations and averaged. Error bars represent standard deviation between replicates.

Figure S9

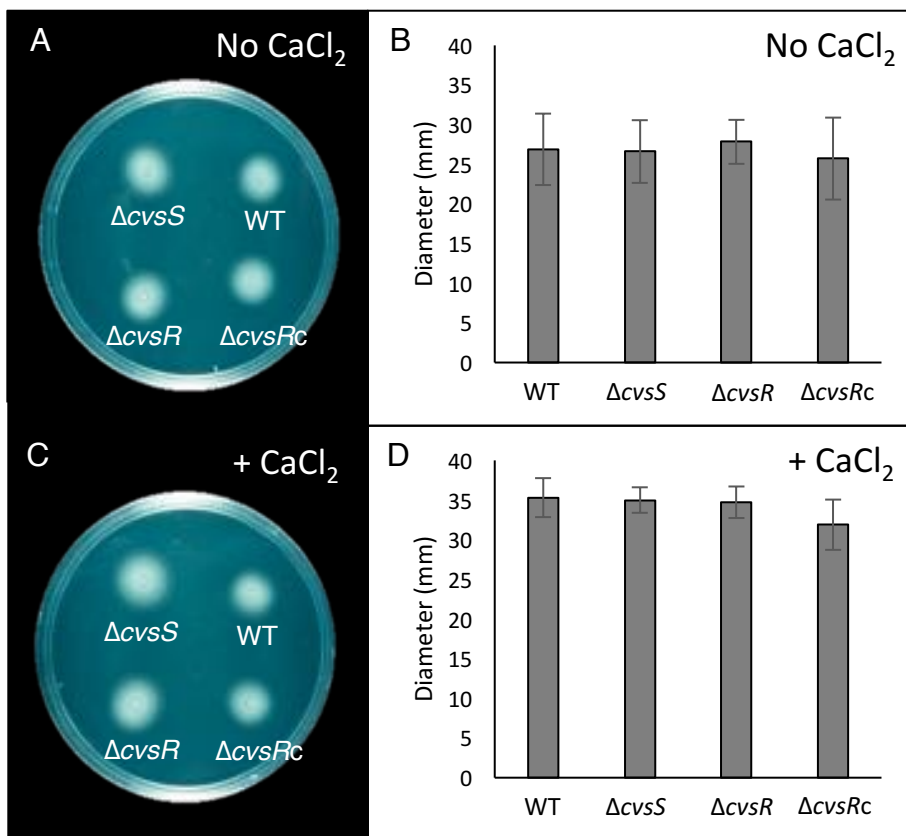


Fig. S9: Swimming assays of WT, $\Delta cvsS$, $\Delta cvsR$, and $\Delta cvsRc$ strains grown on swimming media. (A) Picture of strains taken two days after the start of a swimming assay without $CaCl_2$. (B) Diameter of swimming by strains in swimming media taken two days after the start of the assay. (C) Picture of strains taken two days after the start of a swimming assay with $CaCl_2$. (D) Diameter of swimming by strains in swimming media with $CaCl_2$ taken two days after the start of the assay. Pictures of the plates are representative of swimming assays that were performed three times. The diameters are averaged from three biological replicates. The error bars represent standard deviation across from the three biological replicates.

Fig. S10

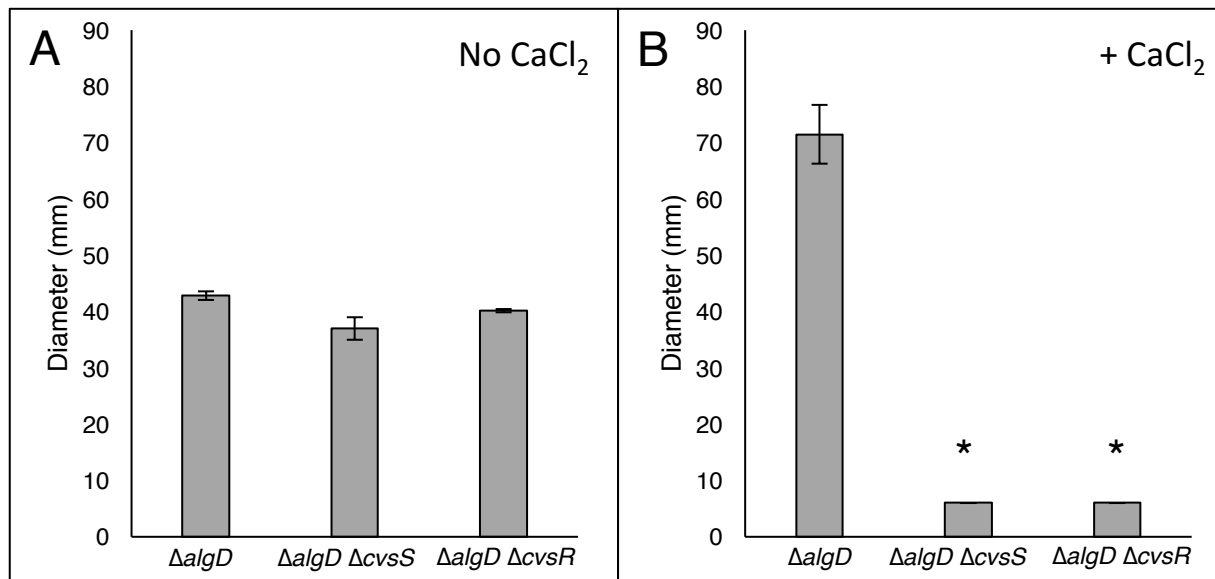


Fig. S10: Diameters of swarming colonies for $\Delta algD$, $\Delta algD$, $\Delta cvsS$, and $\Delta algD \Delta cvsR$ strains measured 24 hours after spotting on (A) NB or (B) NB supplemented with $CaCl_2$. Diameter of colonies was measured across two locations and averaged. The experiment was performed three times with three replicates per experiment. The graph is from a single experiment and is representative of trends observed in each experiment. Error bars represent standard deviation between replicates. The * denote a statistically significant difference with a p-value < 0.01 in swarming diameter between $\Delta algD$, $\Delta algD$, $\Delta cvsS$, and $\Delta algD \Delta cvsR$ strains.

Fig. S11

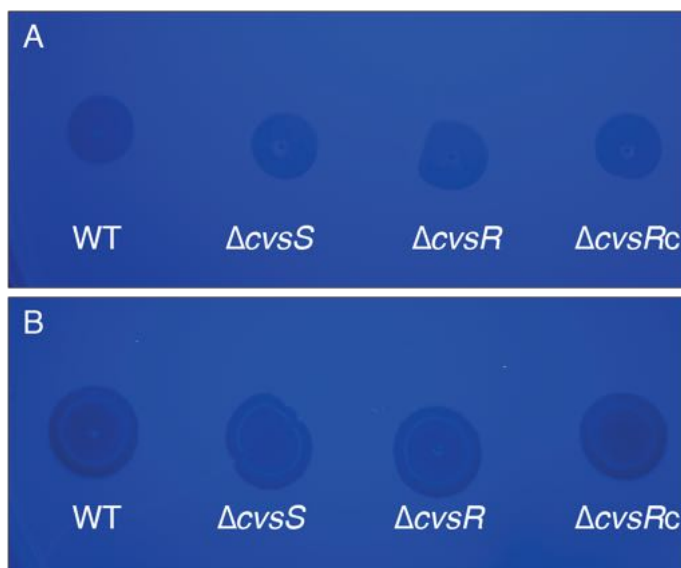


Fig. S11: Growth of WT, $\Delta cvsS$, $\Delta cvsR$, and $\Delta cvsRc$ on NB supplemented with CW after 16 hours (A) and 3 days (B) of growth. Fluorescence of the bacterial strains under ultra-violet light indicated production of cellulose. Bacterial strains were grown to stationary phase in KB media were resuspended at an OD_{600} of 0.3 in NB media and then five μ L of each culture were spotted onto the appropriate media. The plate is representative of assays that were performed three times.

Fig. S12

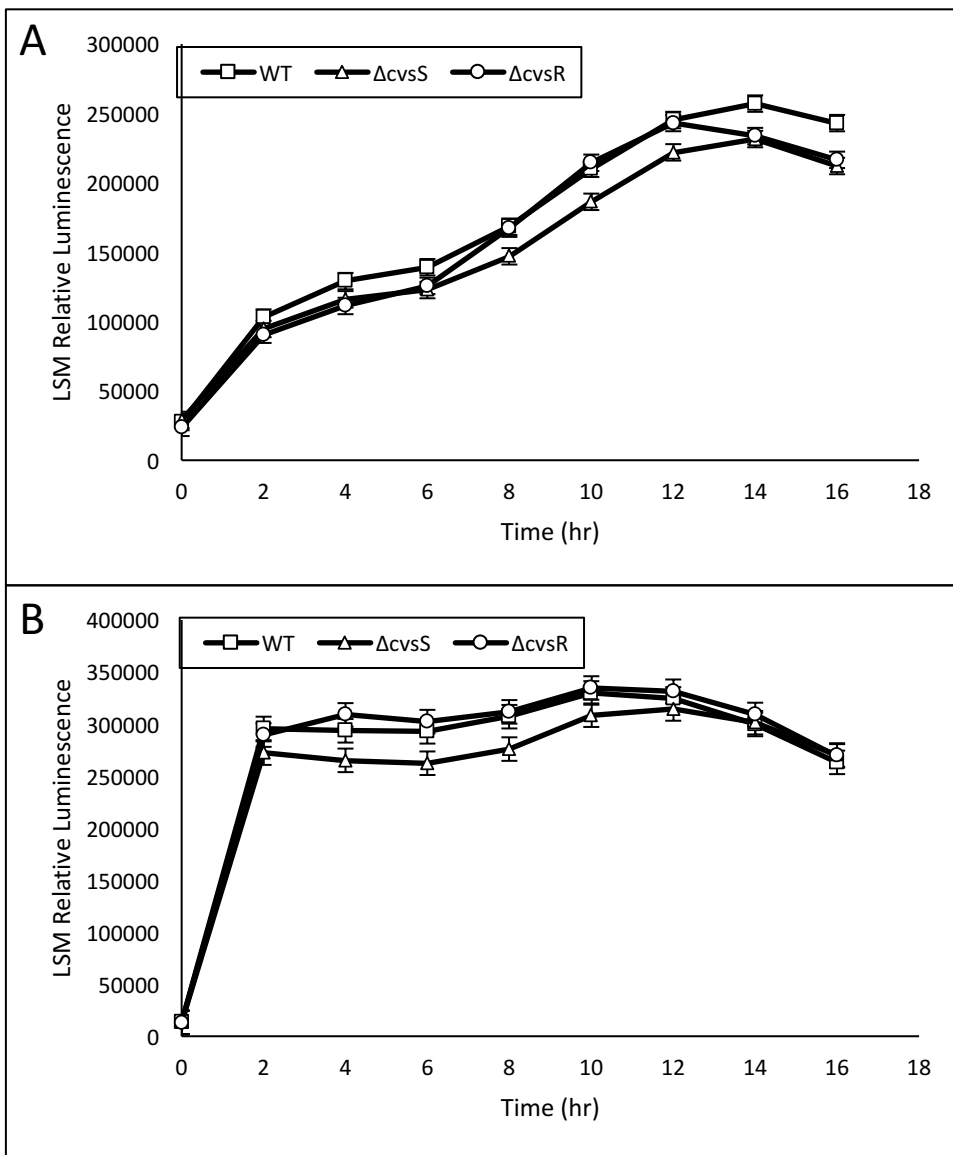


Fig. S12: Luminescence assay to assess transcription of (A) P_{hrpRS} and (B) P_{hrpL} in WT, the $\Delta cvvS$, and the $\Delta cvvR$ when grown in MG. The relative luminescence was calculated using the total luminescence relative to OD_{600} . This experiment was independently replicated three times. The three independent experiments were compiled using a least-squares regression. The error bars represent standard error generated by the differences observed between samples.

Fig. S13

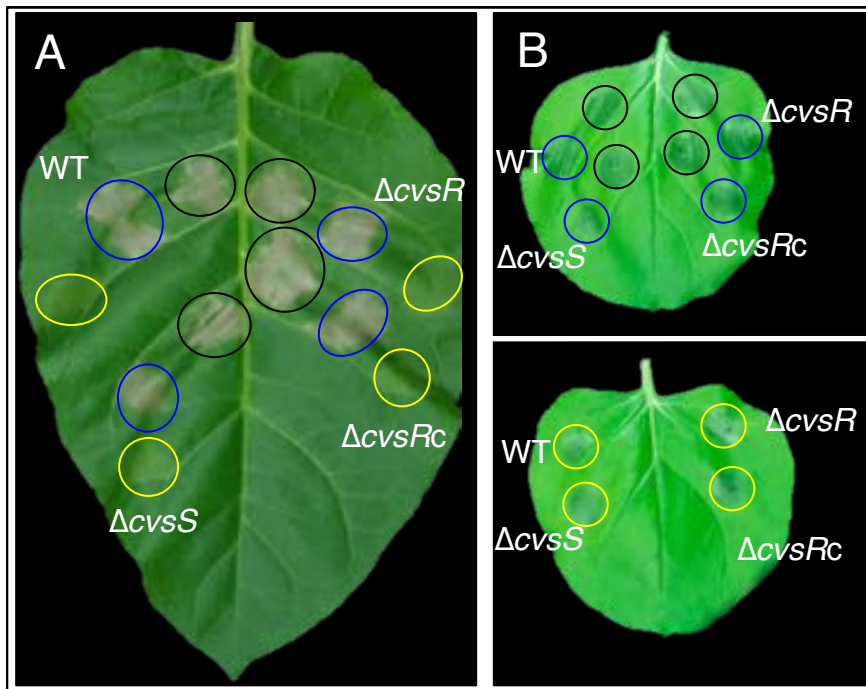


Fig. S13: (A) HR in *N. tabacum* to WT, $\Delta cv s S$, $\Delta cv s R$, and $\Delta cv s R c$ from *Pto* strains at 2×10^8 (black), 2×10^7 (blue), and 2×10^6 (yellow) cfu/mL. (B) HR in *N. benthamiana* with the same *Pto* strains using the same amount of inocula as in *N. tabacum*. Bacterial strains that were inoculated at the same level of inoculum are circled with the same color. The images shown were photographed 2 days after inoculation for *N. tabacum* and 1 day after inoculation for *N. benthamiana*. The experiment was repeated three times.

Figure S14

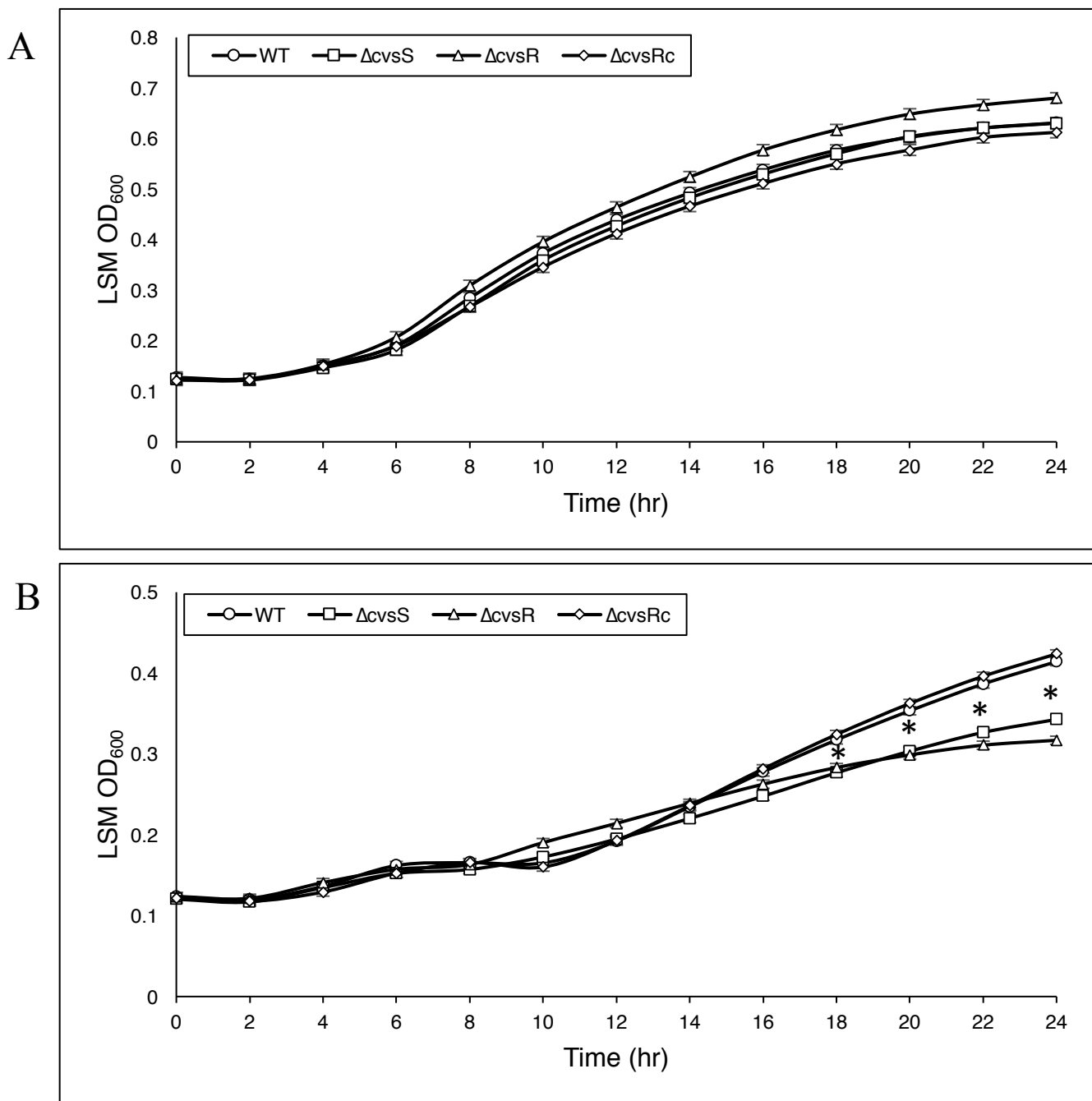


Fig. S14: The least-squares mean of three separate growth curves of WT, $\Delta cvsS$, $\Delta cvsR$, and $\Delta cvsRc$ grown in (A) MG or (B) MG supplemented with Ca^{2+} . The * denotes statistically significant differences determined using a Tukey HSD test with a p-value < 0.01 between OD_{600} of WT, $\Delta cvsS$, and $\Delta cvsR$.

Figure S15

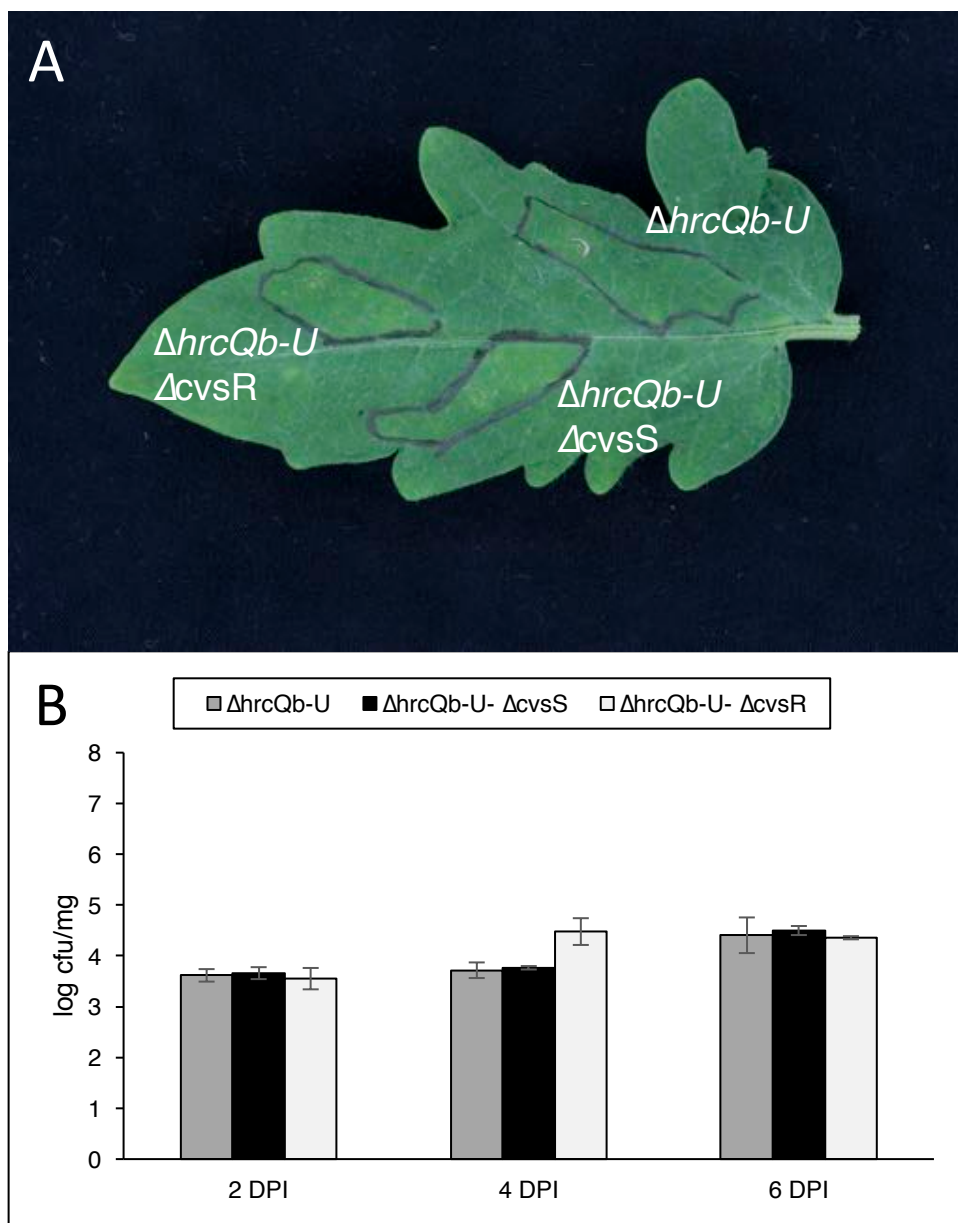


Fig. S15: (A) Picture of syringe infiltrated leaf of tomato at 6 DPI. Areas infected with $\Delta hrcQb-U$, $\Delta hrcQb-U \Delta cvrS$, and $\Delta hrcQb-U \Delta cvrS$ are labeled as such (B) Growth curves over time in log cfu/mg are shown for $\Delta hrcQb-U$, $\Delta hrcQb-U \Delta cvrS$, and $\Delta hrcQb-U \Delta cvrS$ infecting tomato at 4 DPI and 6 DPI. The strains were inoculated at 1×10^6 cfu/mL using a blunt syringe. Average bacterial growth in three plants was used with the error bars representing the standard error between the three replicates.